DOI:10.1021/jf804019x

JOURNAL OF AGRICULTURAL AND FOOD CHEMISTRY
ARTICLE

Development of a High Methoxyl Pectin Edible Film for Retention of L-(+)-Ascorbic Acid

Carolina D. Pérez,[†,‡] Silvia K. Flores,[†,‡] Alejandro G. Marangoni,[§,∥] Lía N. Gerschenson,[†,‡] and Ana M. Rojas*[,†,‡]

[†]Departamento de Industrias, Facultad de Ciencias Exactas y Naturales, Universidad de Buenos Aires, Ciudad Universitaria, (1428) Buenos Aires, Argentina, [‡]Member of the National Scientific and Technical Research Council (CONICET), Argentina, [§]Professor, and [∥]Canada Research Chair, Food and Soft Materials Science, Department of Food Science, University of Guelph, 50 Stone Road East, Guelph, ON N1G2W1, Canada

An edible film to carry L-(+)-ascorbic acid (AA) was formulated for natural antioxidant food protection. Considering previous works where films based on the "rigid" structure of gellan (deacylated) or on a mixture of acylated−deacylated (more "disordered") gellan were used for network development, pectin was herein chosen by considering that the alternating presence of "disordered" (hairy) regions together with ordered (homogalacturonan) ones could sufficiently immobilize water for better AA retention and lower browning. High methoxyl pectin (HMP) was first investigated. AA stability and browning were studied during film storage at 33.3, 57.7, or 75.2% relative humidity (RH) and 25 °C; their dependence on water mobility determined through ^{1}H NMR analysis as well as the correlation between browning and AA degradation were again found. Network characteristics and glycerol (plasticizer) interactions were analyzed through X-ray diffraction and Fourier transform infrared spectroscopy as well as through uniaxial tensile assay. From all results obtained, it was hypothesized that browning development in solidlike systems may be directly related to the water molecules more closely adsorbed on the hydroxyl−polymeric (active) surfaces. The HMP film microstructure produced the best immobilization of water molecules except at 75.2% RH, where it showed lower AA stability than acylated−deacylated gellan film. It is suggested that disordered regions of this pectin network may not be adequately counterbalanced by more transient junction zones of alternating hydrophilic (water) and hydrophobic (methyl ester) interactions, also disturbed by glycerol molecules, for accomplishing enough water immobilization in the whole network at 75.2% RH.

KEYWORDS: Edible film; ascorbic acid; high methoxyl pectin; browning; water

INTRODUCTION

In the past half century, synthetic petroleum-based polymers have been widely used in a variety of packaging materials but have become a major source of waste disposal problems due to their poor biodegradability. With the increasing demand by consumers for high-quality foods and concerns about limited natural resources and the environment, the use of renewable resources to produce edible and biodegradable packaging materials that can improve product quality and reduce waste disposal problems is being explored. Biopolymer-based edible films and coatings are intended to function as barriers against moisture, oxygen, flavor, aroma, and oil, thereby improving food quality and enhancing the shelf life of food products (*1*).

Water-soluble polysaccharides are commonly used in food-related applications as thickeners due to their increase in viscosity when hydrated (*2*−*4*). Polysaccharides can also constitute edible films, an important quality since these polymers are of natural origin, come from renewable sources, and are biodegradable as well. Although it is recognized that polysaccharide edible films are not good barriers against water vapor, they can find interesting applications as food interfaces (*5*), as carriers of active compounds or preservatives (*6*), constituting delivery systems with local activity (*7*−*9*).

Edible films based on gellan polymers, the deacylated form of the gum secreted by *Sphingomonas elodea*, have already been developed to support L-(+)-ascorbic acid (AA) for antioxidant protection of foods, by leveraging its natural activity as a vitamin in human metabolism (*10*, *11*). Kinetics of AA destruction at the prevailing anaerobic condition of storage and of the subsequent nonenzymatic browning (NEB) development were studied in these previous works at 33.3, 57.7, and 75.2% relative humidity (RH), and their relationship with the microstructure, at the macromolecular and molecular levels, was also analyzed. The important compromise of water availability in AA degradation at anaerobic storage and in NEB as well was observed, since the first

*To whom correspondence should be addressed. Tel/Fax: +54 11 4576-3366. E-mail: arojas@di.fcen.uba.ar.

 Published on Web 07/17/2009

reaction of AA at this condition involves its hydrolysis to diketogulonic acid (DKG). It was suggested that browning may just begin from the latter product, favored by the relatively low RH (or a_W) of storage, which allows dehydrations involved in the browning reaction chains in solidlike systems (*10*). It was suggested that local water mobility at a constant RH value may be connected with the local microstructure of the film network. Gellan is constituted of a parallel, half-staggered, double helix stabilized by both intra- and interchain hydrogen bonds. The flexibility of the chain is tempered by three bonds per tetrasaccharide monomer of glucose (Glc), glucuronic acid, Glc, and rhamnose (Rha) (*12*). The gellan network would be a continuous branched fibrous structure showing fibers of variable thickness, which results after side-by-side association or lateral aggregation of helices. Hence, the junction zones are continuous throughout the gel network due to the presence of free carboxyl groups. Without "disordered" regions, the elasticity of the gellan gel will be due to the bending and stretching of fibers (*13*). It was then hypothesized that this "rigid" network cannot immobilize water sufficiently for promoting higher AA stability and lower NEB development. Hence, it was suggested that the presence of glycerate and acetyl side chains in the gellan chains by using a mixture of gellan and of its acylated form would lead to a film network where lateral aggregation would be hindered, producing a less rigid network, which may contribute in some degree to better immobilization of water. This also permitted, as expected, the usage of a lower proportion of glycerol for adequate film flexibility. This film network determined higher AA retention and lower NEB development with similar mechanical characteristics (*11*, *14*). The above hypothesis led us to also think about pectin as a convenient polymer to constitute film networks when polysaccharides are selected for film making. Pectin is a structural component of cell walls, which consists primarily of partially methyl esterified poly α-D-1,4-linked galacturonic acid (homogalacturonan, "smooth" ordered regions), but it also shows kinks of (1→2)-linked α-L-rhamnose residues with remaining "hairy" regions due to side chains of arabinogalactan I, which constitute the disordered regions in the commercial product (*13*, *15*−*17*). As a first approach, a high methoxyl (73% esterified) pectin was then selected in the present paper for film development, looking for better AA retention as well as a lower browning rate as a consequence of controlled water mobility in the pectin network.

MATERIALS AND METHODS

Safety. This research work was performed in accordance with the Safety Protection Plan of the Facultad de Ciencias Exactas y Naturales of the University of Buenos Aires, where the laboratories are periodically submitted to the inspections of the Department of Hygiene and Safety.

Chemicals. Food grade pectin with a high degree of methylation (GENU pectin type B rapid set-Z) for manufacturing foodstuffs was from CP Kelco (J. M. Huber Corp., Edison, NJ). Its relevant molecular characteristics are listed in **Table 1**. It contains negligible amounts of divalent cations and a higher content of sodium and potassium. All other chemicals were of analytical quality from Merck (Buenos Aires, Argentina) or Sigma (St. Louis, MO).

Preparation of Films. Films were made using casting technology. An aliquot of 6 g of the high methoxyl pectin (HMP) powder was slowly poured in 260 g of continuously stirred deionized water under controlled high speed shear (vertical stirrer model LH, Velp Scientifica, Italy), to reach homogeneous hydration of the powder to avoid lumps. While the high speed stirring was performed, the obtained viscous, homogeneous, and transparent system was then heated to 90 °C at a constant heating speed (5 °C/min) on a hot plate, with simultaneous recording of the temperature every 20 s through a thermocouple connected to a Consort millivoltmeter (P 901, CE Belgium). Glycerol was added (3.5 g) as a plasticizer, followed by potassium sorbate (0.03% w/w) and AA (0.100% w/w), both predissolved in deionized water. The total weight of the system was then made to 300.00 g by adding enough deionized water, followed by stirring for homogenization. The film-forming solution presented a pH of 3.16 when measured at 25 °C. The hot solution was placed under vacuum for 20 s to remove air bubbles and immediately poured onto leveled polystyrene plates. They were cooled for 60 min at room temperature, but gelation was not observed in the pectin solution contained in the plates. After this, the fractionated system was air-dried in a convection oven for 2.5 h at 60 °C. After they were cooled to room temperature, films were peeled from the polystyrene plates and stored over saturated solutions of known water activity (a_W°). Salts used in the solutions were as follows: $MgCl_2$ (a_W° = 0.333), NaBr (a_W° = 0.577), and NaCl (a_W° = 0.752) at 25 °C. Equilibration was assessed by measurement of a_W values of film samples every day until that of the saturated solution used was attained. Afterward, the sample thickness was measured to the nearest 0.001 mm using a digital micrometer (Mitutoyo, Kawasaki, Japan) at six different locations in each of 10 specimens. For kinetic studies, samples were collected during storage. In general, three batches of films (replicates) were prepared as indicated, and each one was stored at RH for the influence of film making to be allowed for consideration in the study. The following analyses were performed on samples of the three batches for each time of interest.

Dosage of AA. Each film sample was first cut into pieces smaller than 1 mm in size, weighed on an analytical scale (0.0001 g), and extracted for 1.5 h at 5 °C with a 1% (w/v) oxalic acid solution under magnetic stirring into a 25.00 mL volumetric flask. During this time, it was submitted to vortexing (Velp, Italy) for 90 s at 35 Hz every 15 min. The suspension was finally centrifuged at 10000 rpm and 6 °C for 30 min (Eppendorf 5810R Refrigerated Centrifuge, United States). An aliquot was taken from the supernatant, and the AA concentration was determined through the 2,6-dichlorophenol indophenol (2,6-DPIP) spectrophotometric method (*10*) in duplicate for each sample.

Determination of pH. It was performed on the gel-forming solutions as well as on the films after their equilibration at the corresponding RH, as previously indicated (*11*).

Water Activity. It was determined on film samples with a Decagon's Aqualab (Series 3 Water activity meter, United States) at 25 °C (constant temperature), according to León et al. (*11*).

Color Evaluation. Film disks of 20 mm diameter were used for color measurement in a Minolta colorimeter (Minolta CM-508d, Tokyo, Japan) using an aperture of 1.5 cm diameter, as previously explained (*11*). The yellow index (YI) parameter was measured for reporting the NEB developed in film samples, according to ASTM D-1925 (*18*).

Moisture Determination. Films were sampled at various time intervals during storage, cut into pieces smaller than 1 mm in size, weighed (0.0001 g), and placed into small, light glass containers. They were then frozen in liquid nitrogen and freeze-dried at room temperature for 48 h (Christ, Freeze-Dryer Alpha 1-4 LD, Germany, and a Pfeiffer vacuum pump, Duo 5M, Germany), as previously reported (*10*). As in the case of performing moisture determinations through a vacuum oven at 70 °C until constant weight for around 30 days (*10*), the freeze-dried samples obtained were immediately led for 48 h into a chamber under P_2O_5 to follow the same protocol. Statistical differences were not found in the moisture contents obtained through both methods as in previous assays. Hence, we preferred to freeze dry not only for rapidness but also because sample chemical composition essentially does not change during dehydration at low temperatures. Determinations were performed on six film specimens from each evaluated condition.

Glass Transition Temperature. Differential scanning calorimetry (DSC, 822^e Mettler Toledo calorimeter, Schwerzenbach, Switzerland) was used to determine the T_g (onset value) of the second scan performed as previously indicated (*10*, *11*). It was calibrated with the melting points of indium (156.6 °C), lead (327.5 °C), and zinc (419.6 °C), in addition to the DSC periodic calibration performed with a sapphire disk, in the whole temperature range where the equipment is usually employed (*19*).

Fourier Transform Infrared Spectroscopy (FTIR) Spectroscopy. FTIR spectra were recorded at ambient temperature and atmospheric pressure on a Nicolet 8700 (Thermo Scientific Nicolet, MA) spectrometer, which was equipped with a diamond attenuated total reflection (ATR) device, a DTGS TEC detector, and a reflection incident angle of 45°. Each

Table 1. Molecular Characteristics of the HMP[a] Used for Film Constitution

		%				
molecular mass ($\times 10^3$ Da)[b]		total carbohydrate content[b—d]	galacturonic acid[b,c]	degree of methylation[b,c,e]		degree of acetylation[b,c,e]
457 (204−684)[f]		98 ± 1	82 ± 3	73 ± 2		14 ± 2
		neutral sugar composition[b] (mol/100 mol)				
Rha	Fuc	Ara	Xyl	Man	Gal	Glc
13.2	0	36.6	1.9	0	44.1	4.2
		cation content[g] (mol/100 g)				
Na		K	Ca			Mg
1.870×10^{-2}		9.49×10^{-3}	3.75×10^{-3}			1.47×10^{-3}

[a] The same composition was shown by the commercial HMP as well as after dialysis through a membrane with a molecular weight cutoff of 12000 (Sigma) (*17*). [b] Chemical assays and molecular weight analysis were performed according to Fissore et al. (*17*). [c] Means and SDs (n = 3) are shown. [d] Total carbohydrates are expressed as g of galacturonic acid (standard for calibration curve) per 100 g of product (*17*). [e] The degree of methylation was calculated as the molar ratio with respect to the galacturonic acid content, whereas the degree of acetylation was the molar ratio with respect to the total carbohydrate content. [f] The molecular weight range is also shown. [g] The cation content was determined through atomic absorption spectrometry (*17*).

spectrum was obtained by recording reflectance (%) through 64 scans performed with a resolution of 4 cm^{-1} and between 4500 and 525 cm^{-1}. Spectra were analyzed through the OMNIC software (version 7.3, Thermo Electron Corp., United States).

Nuclear Magnetic Resonance (NMR) Proton Mobility. All of the experiments were performed on film samples using a Bruker Avance II spectrometer operating at 300 MHz for 1H. The probe was a Bruker high power CPMAS and was used under static conditions. The rotor sizes were 18 mm long with a 4 mm outer diameter. All of the experiments were conducted on resonance at room temperature, in triplicate as previously explained (*10*, *14*).

X-ray Diffraction. A Philips X-ray diffractometer with vertical goniometer was used (Cu Kα radiation λ = 1.542 Å). Operation was performed as previously indicated (*10*). The order of reflection (n) was considered as 1 for calculation.

Water Vapor Permeability (WVP). It was determined following the procedure and calculations indicated by Gennadios et al. (*20*) for hydrophilic films, by taking into account the resistance of the air column to the vapor transference in the space (10 mm) remaining between the calcium chloride desiccant placed into the cup and the film sample at the top of the beaker, which was in contact with an environment of 73% RH at 25 °C (Ibertest chamber, Spain).

Tensile Test. The tensile strength (N/m) was calculated as the ratio between the tensile force (N) and the corresponding extension or deformation (m) at failure, determined from the force-elongation curves recorded at 5 mm/min constant crosshead speed in an Instron Testing Machine (model 3345, Norwood, MA), as previously explained (*11*).

Atomic Force Microscopy (AFM). This study was performed on film samples under a nitrogen atmosphere, by taking images through an atomic force microscope (NanoScope III, Digital Instruments, CA) and performing image analysis (*21*) with the scanning probe microscopy software WSxM 4.0 Develop 11.3-Package (2007, Nanotec Electronica, Spain), as previously indicated (*14*).

Microstructural Parameters. The tensile strength at failure (T_s) was found to be related to the volume fraction of network solids (ϕ) in a power law fashion:

$$T_s = A \cdot \varphi^m$$

This power law dependence was assumed to arise due to the fractal arrangement of polymer particles in aggregates. In the weak-link rheological regime where the elastic constant of the flocs is much greater than the elastic constant of the links between the flocs, $m = 1/(3 - D_f)$, where D_f is the fractal dimension for the arrangement of particles within the flocs (*22*). The fractal dimension of the gels was determined by equilibrating the films at each RH and finding their tensile strength at failure for each of these HMP concentrations with different moisture contents. Measurements were made in at least six different samples from each condition. The slope of the log−log plot of T_s vs ϕ corresponds to m, which can then be used to determine D_f assuming the weak-link rheological regime as stated above.

Image analysis of atomic force micrographs was performed using Adobe Photoshop 5.5 (Adobe, United States) and Fovea Pro 3.0 (Reindeer Graphics, Asheville, NC) to determine the Euclidean distance map (EDM) fractal dimension (D_{EDM}) as explained in J. C. Russ's Image Processing Handbook (*23*). Atomic force micrographs were converted to 8-bit grayscale images and inverted using Adobe Photoshop CS (version 8.0.1) (mass was black), while thresholding was carried out using the Fovea Pro filters.

Statistical Analyses of Data. The results are reported as the average and standard deviation (SD). Rate constants of AA destruction were calculated by linear regression where AA concentration was in terms of g AA/weight (g) of the corresponding film sample assayed. Analyses of covariance (ANCOVA) were applied for the comparison of slopes, that is, rate constants, as indicated by Sokal and Rohlf (*24*). The statistical analyses of results were performed by applying ANOVA (α: 0.05), followed by pairwise multiple comparisons evaluated by Tukey's significant difference test (*24*). The significance of linear correlations was evaluated according to Bancroft (*25*). The GraphPad Prism software (version 5.00, 2007, GraphPad Software Inc., United States) was used for all analyses previously detailed.

RESULTS AND DISCUSSION

Homogeneous and flexible films were obtained after casting from the solution containing HMP with the degree of esterification reaching 73% (**Table 1**) and were plasticized by glycerol [glycerol·100/(pectin + glycerol) = 36.84% w/w]. They showed transparency and slight yellowness (b = +8.90; YI = 16 ± 3 YI units), as well as high initial lightness (L = 86.0% ± 0.2). All films were easily removed from polystyrene cast plates after 20 min of cooling at room temperature. The initial AA concentration was ≈3.03% (w/w) on a film basis, which accounted for ≈100% of AA retention after casting. Film samples were stored at 25 °C. Equilibration was reached at the fourth day of storage at each condition of RH, as indicated through measurement of the film water activity every day.

A constant pH of 3.70 ± 0.09 was found during film storage at each RH (33.3, 57.7, or 75.2%) assayed, as well as a thickness of 0.15 ± 0.03 mm, after equilibration. Moisture contents were between 16.6 and 26 g water/100 g of a film's dried mass (**Table 2**).

X-ray. The X-ray diffraction patterns of material showed essentially an amorphous structure with only two detectable intensities in the regions of 2θ = 15.81° (d spacing, ≈ 5.6 Å) and 2θ = 28.87° (d spacing, ≈ 3.1 Å), which were especially evident in films stored at 33.3 or 57.7% RH (**Figure 1A**,**B**). Other detectable intensities were also observed in the region of 2θ = 6.81 and 7.98° (d spacing, ≈ 12.98 and 11.08 Å, respectively). The existence of some crystalline regions can be ascribed to well-ordered binding

Table 2. Parameters Determined on High Methoxyl Pectin Films Stored at Constant RH and 25 °C[a]

	RH (%)		
	33.3	57.7	75.2
k_{AA}'[b] (min^{-1})	$(1.9 \pm 0.2) \times 10^{-6}$	$(2.8 \pm 0.5) \times 10^{-6}$	$(23 \pm 2) \times 10^{-6}$
k_{YI}[b] (YI units min^{-1})[c]	$(1.08 \pm 0.08) \times 10^{-4}$	$(4.6 \pm 0.2) \times 10^{-4}$ [d]	$(13.33 \pm 0.05) \times 10^{-4}$
lightness,[e] L (%)	82 ± 2 A	85.4 ± 0.8 A	85.8 ± 0.2 A
half-shelf life of AA ($t_{1/2}$, d)	250	90	20
time for duplicating YI initial value (t_2, d)	90	35	14
moisture content[f] (g water/100 g dry matter)	16.6 ± 0.6	21.5 ± 0.6	26 ± 1
glass transition temperature (onset), T_g (C)	−84.7	−94.2	−108.4
change in specific heat at the glass transition [J/g (dm) K][f]	0.603	0.371	0.876

[a] The same capital letter in a row means nonsignificant differences ($p < 0.05$). [b] The rate constant and its SD are shown ($n = 3$). [c] YI to report NEB development. [d] Kinetic constant value from fitting experimental data up to 55 days. After this, the YI was constant (53 ± 4) up to 107 days. [e] SDs are shown ($n > 11$). [f] dm, dry matter.

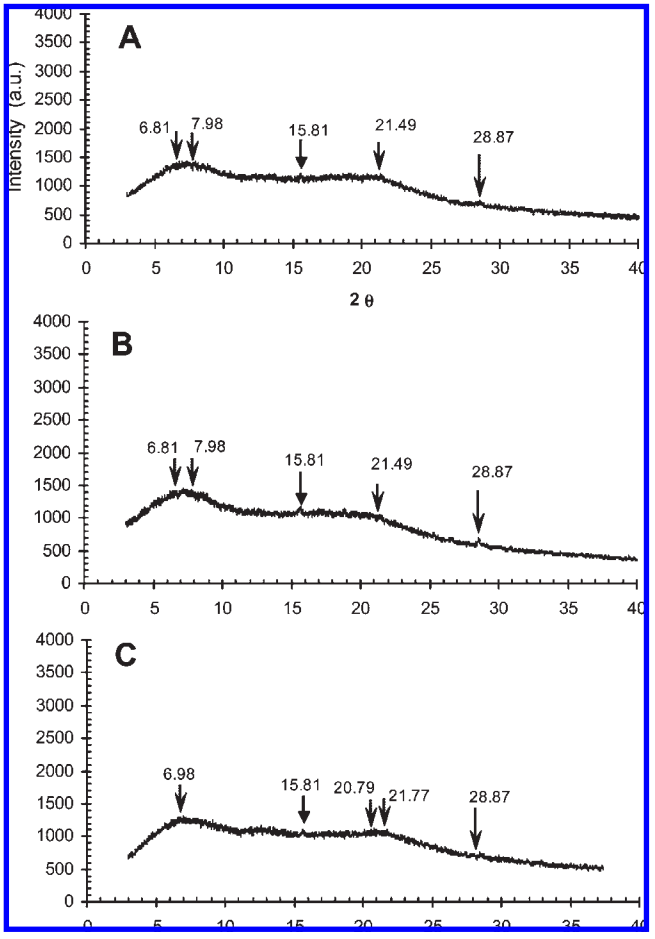

Figure 1. X-ray diffraction patterns of HMP films stored at 33.3 (**A**), 57.7 (**B**), or 75.2% (**C**) RH and 25 °C.

throughout the polysaccharide network (*13*). The X-ray diffraction study of pectic (polygalacturonic) acid reported by Chandrasekaran (*12*) showed interhelical associations of 2.8 Å occurring through direct O3H···O62 and O61H···O6 hydrogen bonds involving the carboxyl groups of the antiparallel related helices. Studies carried out on calcium pectate revealed that pectin macromolecule is a right-handed 3-fold helical conformation where two macromolecules show antiparallel association, through some calcium pectate junction zones, shifted by 1.7 Å, respectively, where some degree of methyl esterification can be accommodated within them by only slight modification of the ester group's torsion angles (*26*). On the other hand, Chandrasekaran (*12*) reported that pectinic acid (100% methylester of polygalacturonic acid) is also a 3-fold helix, but it has a hexagonal packing arrangement with only one helix per trigonal unit cell ($x = y = 8.37$ Å and $z = 13.0$ Å). In this idealized 100% methylester form of pectinic acid, the unit cell has a triangular column of methyl (hydrophobic) groups, enclosed by three helices, and a similar channel filled with water molecules hydrogen bonded to the surrounding polymer chains. The network formed by alternating hydrophobic and hydrophilic channels embedded among the helices provides an interesting motif in the formation of junction zones, which are implicated in the gelation process (*12*), as thermodynamically quantified by Oakenfull and Scott (*27*) in the case of high methoxyl pectins. The latter authors indicated that mainly hydrogen bonds necessarily in conjunction with hydrophobic interactions contribute to the free energy of gelation or formation of junction zones in this kind of pectins. Hence, the free carboxylic groups (27%) of the HMP herein used for films can relate antiparallel helices through hydrogen bonds (2.8 Å), whereas the alternating hydrophobic and hydrophilic channels of the methyl-esterified (73%) poygalacturonic acid ($z = 13.0$ Å) are actually segments (smooth regions) interrupted by some kinks of L-rhamnose (*15*) substituted by lateral chains of D-galactose and L-arabinose (arabinogalactan side chains) and by defects of other sugars like D-xylose and D-glucose (**Table 1**) (*28*). The mentioned kinks of rhamnogalacturonan I and some other sugar defects (e.g., xylogalacturonan) constitute the known nongelling "hairy" regions of pectins, that is, the amorphous (disordered) zones of the polysaccharide film network developed after film casting. Reducing the degree of methylation (to 73% in the present film) with respect to pectinic acid would increase the amount of water within the network formed by the alternating hydrophobic and hydrophilic channels. The addition of cosolute would not only compete for this water but also disrupt the formation of the hydrophobic cage, altering the gelation properties (*12*). Oakenfull and Scott (*27*) determined that the specific function of sugars and polyols in the formation of gels of HMP are to stabilize junction zones by promoting hydrophobic interaction between ester methyl groups. In the present work, pectin swelled in water in the film-forming solution, but gelation was not observed (pH = 3.16). Dehydration in the presence of glycerol in the network during casting, followed by the increase in the moisture content during storage, led to a solidlike system because the concentrated glycerol, like a cosolute, may have contributed to the stabilization of the hydrophobic interaction between methyl groups during dehydration but avoided the complete reorganization as a polymer−polymer interactive network of alternating hydrophobic and hydrophilic (water) channels at the junction zones, leading to an essentially amorphous material (**Figure 1**). In this sense, Chandrasekaran et al. (*29*) indicated that glycerol can produce disturbance of filament aggregation in the case of gellan polymer.

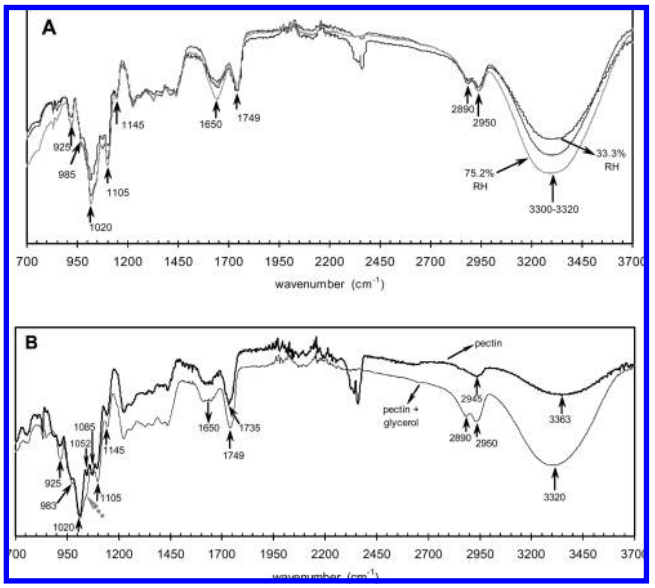

Figure 2. (**A**) FTIR spectra of HMP films stored at 33.3 (black line), 57.7 (gray line), or 75.2% (light gray line) RH and 25 °C. (**B**) FTIR spectra of films made only with HMP (called "pectin"; black line) and with the addition of glycerol (called "pectin + glycerol"; light gray line), which were stored at 0% RH; gray arrow indicates the broadening of the 1020−1022 cm^{-1}-band.

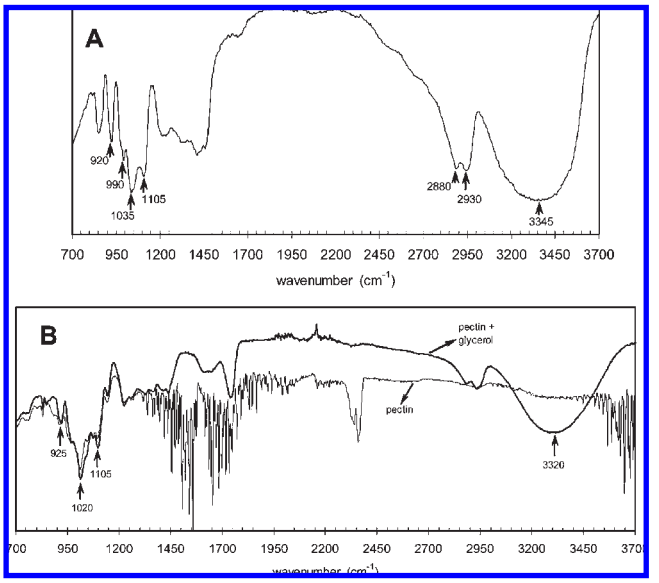

Figure 3. (**A**) FTIR spectra of glycerol and (**B**) films made only with HMP (called "pectin"; black line) and with the addition of glycerol (called "pectin + glycerol"; light gray line), which were stored at 33.3% RH.

FTIR. FTIR spectra of films that were stored at constant RH can be seen in **Figure 2**. The signals at typical wavenumbers corresponding to pectin polysaccharide can be observed, like the band in the zone attributed to C═O stretching of the esterified carboxyl group at 1749 cm^{-1}, which occurs as a single major band. It was slightly higher than the broader band manifested at 1615−1650 cm^{-1} by the carbonyl stretching of the carboxylic (nonesterified) group at 33.3 or 57.7% RH, which was coherent with HMP. Although a decrease in this carboxylic group band area is reported to be observed with an increasing degree of pectin esterification, it is not necessarily correlated with the result of quantitative analytical methods because carboxylic group stretching also occurs at another different spectral region (≈1400 cm^{-1}), as indicated by Gnanasambandam and Proctor (*30*). A higher proportion of available water at 75.2% RH of film storage seemed to intensify the band at 1650 cm^{-1}, that is, the C═O stretching movement. Probably, this may be due to a lower compromise of C═O group in hydrogen bonding with O3 of the pectin antiparallel chain when water is more available. Wilson et al. (*31*) reported a water deformation band at 1640 cm^{-1} as corresponding to water adsorbed (δ HOH) on pectin, while carboxylic band was assigned by them at 1605 cm^{-1}. In our work, C═O stretching band may then be sharpened by the signal of adsorbed water.

The characteristic peaks of the polygalacturonic backbone in the fingerprint zone (1200 to 900−850 cm^{-1}) of pectins appear at 1020 and 1105 cm^{-1} (*32*). Characteristic pectin bands are also present in this region corresponding to C−H stretching in the carbohydrate backbone. Pectic samples are characterized mainly by the wavenumbers 1145, 1105, 1014, and 952 cm^{-1} (*33*), where 1105 and 1014 cm^{-1} bands are diagnostic wavenumbers of pectic polysaccharides rich in uronic acids. Some of these characteristic bands in the case of pectin film samples can be seen in **Figure 2A**: the asymmetric stretching of the glycosidic link at 1145 (*34*) and 1105 cm^{-1} as well as a shoulder at 985 and a band at 925 cm^{-1}. A film made only with HMP and stored under an anhydrous (0% RH) atmosphere also showed the characteristic bands at 1145 and 1105 cm^{-1} (less intense) as well as signals at 1052 and 1085 cm^{-1} (**Figure 2B**). A sharp band at 1020 cm^{-1}, a shoulder at 983, and a lower intensity band at 925 cm^{-1} were also observed. When glycerol was added to the latter pectin film and also stored at anhydrous condition, it was remarkable to note the higher intensity of bands at 1105 and 1020 cm^{-1} (**Figure 2B**). Indeed, the small peak at 1052 cm^{-1} was completely masked in the presence of glycerol by the broadening of the sharp band observed at 1020−1022 cm^{-1} (**Figure 2B**, arrow). The same phenomenon was in part observed with respect to the original peak at 1085 cm^{-1}. Both signals can be associated to the C−O bond stretching of C−OH and C−O−C groups of carbohydrate chains (*35*). This was also observed in the total film formulation at all storage conditions (**Figure 2A**). The FTIR spectrum of pure glycerol shows sharp and important bands at 1105, 1035, and 920 cm^{-1} (**Figure 3A**). The band observed at 925 cm^{-1} was then intensified due to the glycerol present in the film formulation (**Figure 2A**,**B**).

The different shape of the band recorded at ≈1650 cm^{-1} for pectin and pectin + glycerol films stored at 0% RH was observed (**Figure 2B**), in comparison with the spectra of films elaborated with all components of the formulation assayed in the present work and stored at 33.3, 57.7, or 75.2% RH (**Figure 2A**). Therefore, the effect of water adsorbed in the pectin macromolecules of the latter films must be stressed (*31*), where a sharpening in the water band at 1640 cm^{-1}, as mentioned above, is clearly observed.

A broad shorter band at 2945 cm^{-1} that corresponds to the OH stretching in the carboxylic group can be observed in the spectrum of the HMP film without glycerol and stored at 0% RH (**Figure 2B**). At the same time, a broad typical band at ≈3363 cm^{-1} was also observed, which is reported as characteristic of polysaccharides from cell walls (*33*). When this film sample was stored at 33.3% RH, it was very difficult to take its spectrum because noticeable noise completely masked the signal from the ATR (**Figure 3B**). The latter was associated with the presence of water vapor at the film surface in the analyzed pectin samples. This phenomenon was not observed when glycerol was added to the latter films, either after storage at 33.3% (**Figure 2B**) or, of course, at 0% RH (**Figure 3B**). Consequently, it can be pointed out that water was not able to penetrate the pectin film network for plasticizing or to disrupt polymer−polymer interactions, unless glycerol was present for plasticization, as it was previously observed in gellan films (*10*).

The broad OH stretch band, observed at a frequency of ≈3363 cm^{-1} for pectin film, was slightly shifted to a lower wavenumber (≈3320 cm^{-1}) when glycerol was added to pectin-alone films (**Figure 2B**), showing no difference when the latter material was also equilibrated at 33.3% RH (**Figure 3B**) or in the case of the complete film formulation (**Figure 2A**). At the same time, when glycerol was present, two bands appeared at 2890 and 2950 cm^{-1} coming from C−H (saturated) stretching, characteristic of glycerol: 2880 and 2930 cm^{-1} for this pure compound (**Figure 3A**).

Hence, it can be suggested that stable hydrogen bonds may be formed between glycerol plasticizer and O atom in the C−O covalent bond of pectin polymers (*36*), shown by the broadening at 1020−1022 cm^{-1} as well as by the band shift of the OH stretch. Small but characteristic peaks shown by pectin-alone films at 1052 and 1085 cm^{-1} were masked by the broadening of the sharp band at 1020 cm^{-1}, when glycerol (**Figure 2A**) and the other compounds (**Figure 2A**) of the edible film system were also present in the formation of the pectin polymeric network. At the same time, it can be hypothesized that water coming from the RH of film storage may penetrate into the film network through interaction with the glycerol plasticizer, which has to be previously H-bonded with polymer chains at the C−O covalent bond. It is reported that glycerol interacts favorably with water to strengthen the H-bond network of the solvent (*37*). Dashnau et al. (*37*) determined that water−glycerol hydrogen bonding shifted the OH stretch frequency of water (3406 cm^{-1}, 25 °C) to lower wavenumbers as the glycerol concentration increased until x_{glyc} = 1.00 (3337 cm^{-1}). Moreover, hydrophobic interactions occurring as a consequence of hydration of apolar groups like methyl ones of the HMP enhance water−water (or, in the present case, water−glycerol) hydrogen bonding over the weaker methyl group−water interactions (*38*). On the other hand, glycerol seemed to interact with pectin through its methoxyl groups because the band attributed to C=O stretching of the esterified carboxyl group was observed at 1735 cm^{-1} for the pectin-alone film stored at 0% RH (**Figure 2B**), whereas this band was revealed at 1749 cm^{-1}, while contoured and sharpened in shape, after addition of glycerol (**Figure 2B**). This coincided with that above-mentioned in the discussion of X-ray diffraction patterns, where it was indicated that glycerol present in the films may interfere with the complete reorganization of pectin macromolecules as a polymer−polymer interactive network of alternating hydrophobic and hydrophilic (water) channels at its junction zones. Because stable hydrogen bonds may be formed between glycerol and O atom in the C−O covalent bond of pectin polymers, this fact may disturb the interhelical association through hydrogen bonds in the case of free carboxyl groups of the antiparallel related helices of the pectic acid backbone. If these carboxyl groups were esterified, this hydrophobic interaction would be disturbed and probably this event may be responsible for the contoured and sharpened band observed at a wavenumber of 1749 cm^{-1} in the presence of glycerol.

WVP. WVP was examined at a vapor pressure difference of 0/73% RH difference across the film. A value of $(10 \pm 2) \times 10^{-10}$ g m^{-1} Pa^{-1} s^{-1} was determined at 25 °C, after applying the correction indicated by Gennadios et al. (*20*). These authors reported a WVP of ≈6.2×10^{-10} g m^{-1} Pa^{-1} s^{-1} for methyl cellulose and of ≈5.0×10^{-10} g m^{-1} Pa^{-1} s^{-1} for corn zein films. Values between 0.8×10^{-10} and 1.7×10^{-10} g m^{-1} Pa^{-1} s^{-1} were also reported for hydroxypropyl methylcellulose films, when assayed for 0%/85% RH across the film at 27 °C (*20*), and a WVP of 8.41×10^{-11} g m^{-1} Pa^{-1} s^{-1} for 0%/90% RH and 38 °C (*39*). Yang and Paulson (*40*) found a WVP changing from ≈1.5×10^{-10} to ≈3.0×10^{-10} g m^{-1} Pa^{-1} s^{-1} for gellan films made from 50 to 60% of glycerol [w/w, plasticizer/(plasticizer + gellan)] concentration, respectively, showing the dependence of the WVP on the plasticizer concentration used.

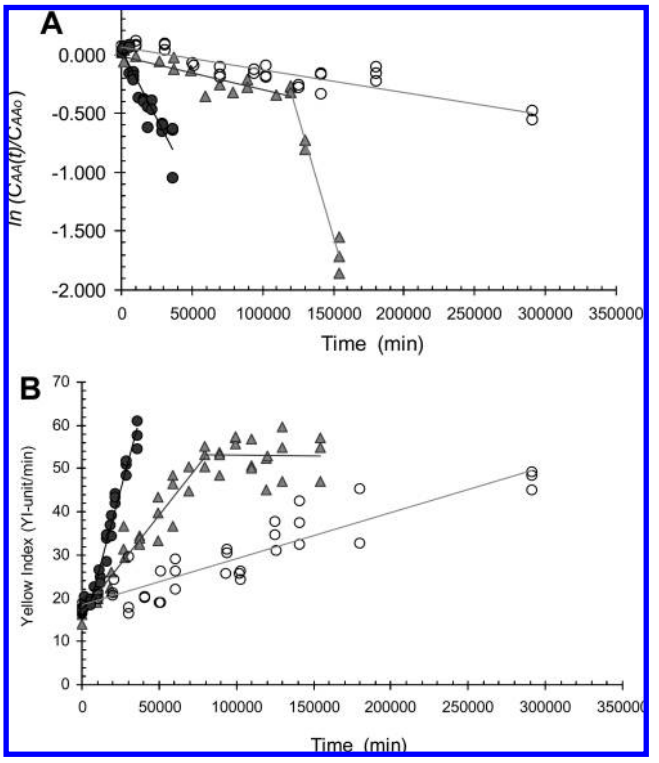

Figure 4. Kinetics curves of AA destruction (**A**) and nonenzymic browning development (**B**) into HMP films stored at 33.3 (○), 57.7 (▲), and 75.2% (●) RH (25 °C). The YI was the parameter used for NEB evaluation.

HMP films were effectively plasticized by glycerol and, secondarily, by water coming from a storage atmosphere, as demonstrated by FTIR assays. Glycerol seemed to interfere in the film polymeric network at the junction zones, increasing intermolecular spacing (*41*), which led to higher permeation of water vapor molecules. Generally speaking, plasticizers reduce intermolecular forces along the polymer chains, thus increasing free volume and chain movements (*41*), as occurs in the case of amorphous HMP films herein studied. Because permeability is the contribution of diffusivity and solubility of the permeance through the solid matrix, the obtained result was coherent with the microstructure developed by the FTIR and X-ray diffraction analyses.

Kinetics of Ascorbic Acid Destruction and Browning Development. The decrease of the ratio between the AA concentration and the initial one with time fit ($p < 0.05$) a pseudo first-order kinetic from zero storage time of films (**Figure 4A**), as earlier reported in the literature for different systems (*42*−*44*). "Equilibration" of the casted films at each water activity, which occurred at ≈4 days of storage, did not seem to affect the kinetic of AA destruction from zero time. Films stored at 57.7% RH showed a breakdown at 83 days, where the rate constant (k_{AA}') increased from 2.8×10^{-6} to 4.1×10^{-5} min^{-1} (**Table 2**). Consequently, half-life times ($t_{1/2}$) of 250, 90, and 20 days were calculated for AA stored at 33.3, 57.7, and 75.2% RH, respectively (**Table 2**). They were, in general, longer than those observed in a previous study for AA entrapped in gellan films ($t_{1/2}$ = 36, 26, and 11 days, respectively) or in film systems based on a mixture of acylated and deacylated gellan ($t_{1/2}$ = 76, 36, and 26 days, respectively), the latter with a similar proportion of glycerol like in pectin films (*11*).

The increment of the YI with storage time statistically fitted ($p < 0.05$) to a pseudo zero-order reaction (**Figure 4B**) as is often

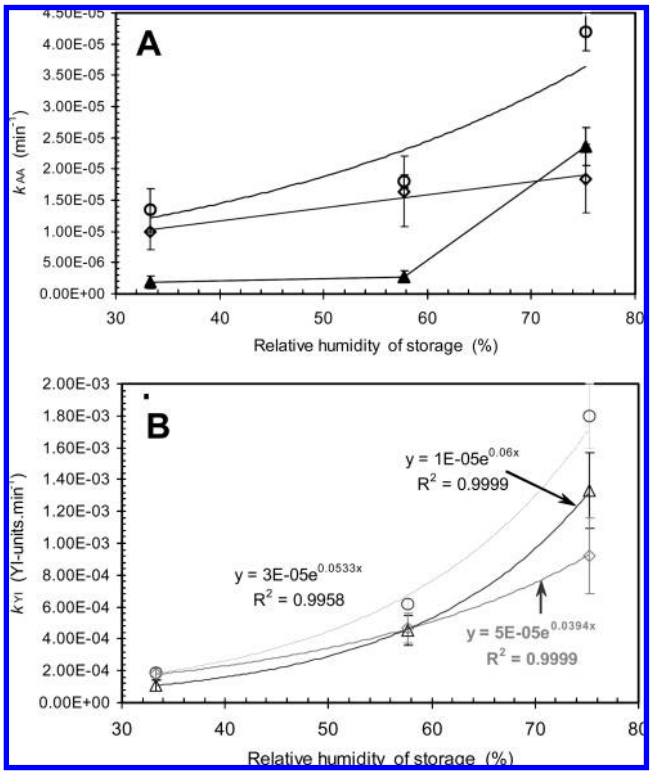

Figure 5. Increase of rate constants for AA degradation (k_{AA}', ▲) (**A**) and nonenzymic browning development (k_{YI}, △) (**B**) measured as the YI against the RH (%) of pectin film storage at 25 °C. The corresponding rate constants determined in a previous study (*11*) in gellan or deacylated are also reported (○) as well as in acylated−deacylated gellan (◇) films.

found in the literature (*45*), once the corresponding lag time (3.88 days) had finished, as occurred in pectin films stored at 75.2% RH. At the fifteenth day of pectin film storage at 57.7% RH, the slope of the browning development changed from a rate constant of 4.6×10^{-4} YI unit min^{-1} to zero, so that a constant value of ≈52 YI units was maintained up to a 21% of AA retention (**Figure 4**). Film lightness (L) was constant during storage at a given RH. Hence, the mean and SD of measured values were reported in **Table 2** for all conditions of RH. The time for YI duplication (t_2) was between 90 and 14 days (**Table 2**).

The rates of AA destruction and NEB development increased with the RH of film storage (**Figure 5A**,**B**, respectively). The browning seems to be associated to AA degradation as indicated through the relationship between $t_{1/2}$ of ascorbic acid degradation and t_2 of NEB (**Figure 6**A). The different AA stability and browning rates at a given RH of storage (**Table 2**) are the result of system composition, as well as microstructure of film network in the presence of the remaining and available water. It was previously proposed (*10*) that water molecules are involved in a S_N2 in the first chemical reaction of AA destruction chain in anaerobic storage, which is prevailing for edible films herein studied (*10*). This reaction leads to hydrolysis of the AA lactone ring to render 2-keto-L-gulonic acid (KGA), through an acid-catalyzed reaction (*46*). The attack of the AA ring by a water molecule (S_N2) was also suggested to be slow enough to determine the total reaction rate. Therefore, the proposed mechanism explains a second-order kinetics for AA hydrolysis (*47*),

$$r_{AA} = -\frac{1}{\nu_{AA}}\frac{d[AA]}{dt} = k[H_2O][AA] = k_{AA}'[AA]$$

Hence, as water concentration takes part of the rate constant (k_{AA}') determined from the measurement of the AA concentration remaining at any time, water availability is then a feature of the pseudo first-order rate constant (k_{AA}') value obtained by statistical fitting of experimental AA data (*10*). Because available water increased as the solidlike (film) networks were stored between 33.3 and 75.2% of RH, k_{AA}' also increased for AA degradation (**Table 2** and **Figure 5**A). Once KGA appears, this reactive molecule (α,β-unsaturated carbonyl, β-hydroxyl carboxyl) suffers successive transformations that involve dehydrations and decarboxylations producing different browning active compounds (*46*). The absence of water available for solvation in the film networks (33.3−75.2% RH range) promotes dehydration reactions as well as high reactivity of nucleophiles (*47*), that is, higher reaction rates of browning than in aqueous solutions of AA and sugars or polyols (*43*). Probably, the null acceleration of browning at the two lowest water contents of films (**Table 2**) can be ascribed to the fact that AA hydrolysis to finally produce KGA was less promoted. This allows conclusion that the latter reaction is in fact a decisive path that controlled the NEB in solidlike systems as pectin films.

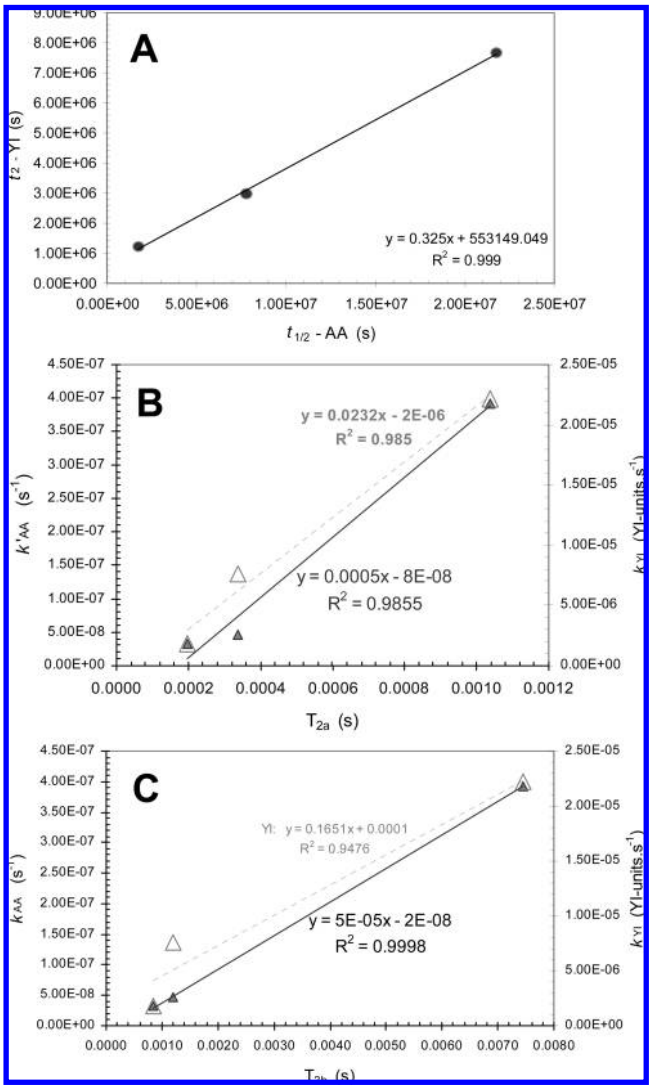

Figure 6. (**A**) Relationship between the time for YI duplication (t_2) and half-time ($t_{1/2}$) of AA destruction. Rate constants of AA degradation (k_{AA}') (▲) and browning development (k_{YI}) (△) vs the spin−spin time constant T_{2a} (**B**) or T_{2b} (**C**). Error bars are in the order of the symbol size.

NMR. Proton (^{1}H) NMR spectroscopy was used to study the dynamic aspects of water interactions in the pectin film network. For low-moisture biopolymer systems (water content < 35%),

the slowing of water motion has been reported to be associated with bound water (i.e., immobile water) arising from hydrogen bonding (*48*). Hence, this is the case for the water dynamics in the present work (**Table 2**). Short-range motions or molecular (water) relaxations investigated through ^{1}H NMR (*49*) led to the observation that the magnetization decay in the *xy*-plane showed two spin−spin time constants (T_{2a} and T_{2b}) as observed after exponential fitting, indicating the existence of multirelaxation rate behavior. These parameters may be associated with two fractions of water, which have different relaxation rates or mobility degrees (*50*, *51*). One of them showed transverse relaxation values between 1.986×10^{-4} and 1.038×10^{-3} s (T_{2a}), while the other water population presented transverse relaxation values ranging from 8.367×10^{-4} to 7.446×10^{-3} s (T_{2b}). It is hypothesized that the latter fraction of water molecules characterized by a higher mobility may be associated to reactive molecules, while the former may probably be related to water compromised on macromolecular plasticization (*11*). Pure water has a T_2 of about 1−2 s, as determined by Chen et al. (*50*).

With different reaction order, NEB kinetics seemed to be more sensible to water dynamics than the AA one (**Figure 6B**,**C**). The rate constants of AA destruction (k_{AA}') and NEB development (k_{YI}) showed the best linear relationship ($R^2 = 0.9998$ and 0.985) against T_{2b} and T_{2a}, respectively (**Figure 6B**,**C**). Thus, AA degradation seems to be mainly involved with the more mobile water population, whereas in the browning development, the slowest water fraction seems to be mainly compromised. It can be hypothesized that in solidlike systems as films herein developed, the hydroxyl groups of pectin macromolecules may be activated as a consequence of adsorption of layers of water molecules closer to the macromolecule surface (*52*). These hydroxyl groups may be involved as active surfaces for water exchange with reactive molecules derived from AA degradation, which leads to the browning development.

Kerr and Wicker (*51*) found limited water mobility in dry pectin samples. These authors determined T_2 time constants ranging from about 100 μs to 400 ms as a function of increasing a_W from 0.11 up to 0.75. Hence, they suggested that there was not a population of water molecules separated by large diffusion distances from the pectin macromolecules. At the same time, they determined that the lowest moisture systems (moisture lower than the monolayer value, which took a value of 11 g H_2O/100 g dry matter) did not have two distinct water (T_2) populations. According to those authors, the monolayer a_W took a value of 0.31, slightly lower than that of 0.333 (33.3% RH) herein used for pectin films. However, it should be kept in mind that the presence of plasticizing substances like glycerol, and others with plasticizing behavior like potassium sorbate (*53*), can contribute to modify the moisture monolayer value in pectin films.

When compared with previously reported results (*11*), HMP films showed significantly lower water mobility (T_{2b} population) and lower AA degradation rates than those determined in gellan as well as in acylated−deacylated gellan films, excepting when pectin films are compared with the latter system stored at 75.2% RH (**Figure 7A**). This result, which was observed when water was more available for reactions, might be attributed to the lower retention of this excess of water molecules in the HMP network. Disorder regions may not be adequately counterbalanced by the more transient junction zones developed in highly methoxylated pectins, since they are constituted by alternating hydrogen bonds and hydrophobic interactions disturbed by glycerol, in which the excess of water adsorbed at 75.2% RH might just not be sufficiently immobilized. However, the AA degradation rate did not increase in the same proportion as in gellan-based (rigid network) films with respect to T_{2b} (**Figure 7A**).

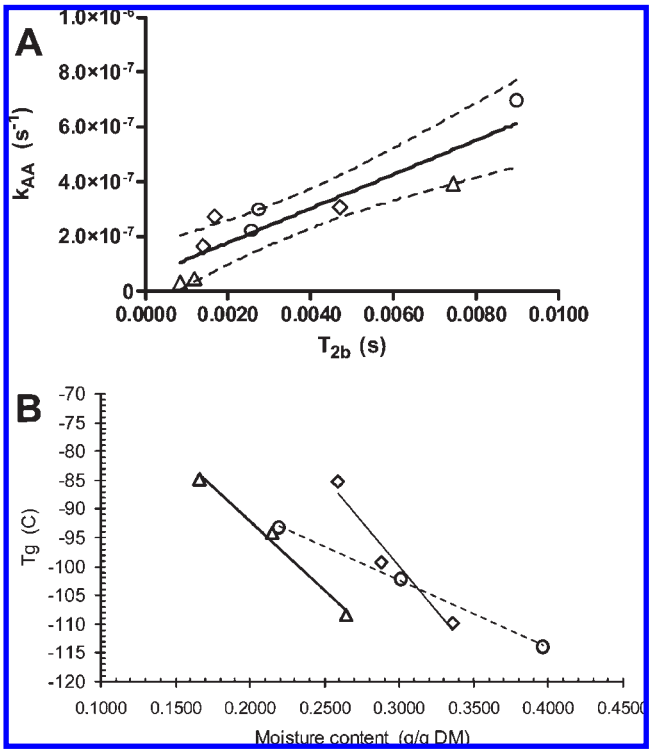

Figure 7. (**A**) Rate constants of AA loss (k_{AA}) against spin−spin relaxation time (T_{2b}) and (**B**) glass transition temperatures (T_g) as a function of the moisture contents of HMP film (△) stored at 33.3, 57.7, or 75.2% RH (25 °C). The same is reported for gellan or deacylated (○) as well as for acylated−deacylated gellan (◇) films (*11*).

The commercial pectin herein used for film making was entirely constituted by carbohydrates (**Table 1**). Disorder (hairy) regions contributed 18% of the total carbohydrate content of the HMP, while the rest was D-galacturonic acid (GalA) with a 73% methyl esterification (homogalacturonan, "smooth" region). A 14% acetylation (mol of acetyl group/mol of total carbohydrates) was also determined. The latter may also contribute to hinder in some degree the structure at the hydrogen bond−hydrofobic-mediated junction zones, modifying or modulating the gelation process (*54*). By considering the composition and molecular weight of the pectin used for films (**Table 1**), it can be assumed from molar ratios (GalA/Rha = 30; [arabinose (Ara) + galactose (Gal)]/Rha = 6) that the pectin macromolecule of 457 kDa could be structurally constituted by ≈49 repeating units of (a) at least 28 molecules of GalA monomers (≈22 of them methylated), followed by (b) another two molecules of free GalA alternating with two molecules of L-rhamnose (rhamnogalacturonan I), the latter two being substituted by two arabinogalactan I side chains of four Gal and 2−3 Ara residues (*55*). The molar ratios of GalA/xylose (Xyl) = 206 and of GalA/Glc = 95 were also considered in the frequency of repeating units. Actually, each 28 residue homogalacturonan region can repeat many times (up to 1372 GalA residues) before to find one chain of rhamnogalacturonan (hairy) region, which will be constituted by repeating units of alternating GalA and rhamnose (up to 196 residues), considering the relative proportions above indicated. The latter means that 14% (molar base) of the pectin network corresponded to amorphous (disorder) regions, while the rest was mainly compromised in the alternating hydrophilic−hydrofobic (transient) junction zones. The pattern of distribution of these regions in the pectin macromolecule as well as of the methyl esterification in the homogalacturonan is also a key factor in the gelation properties

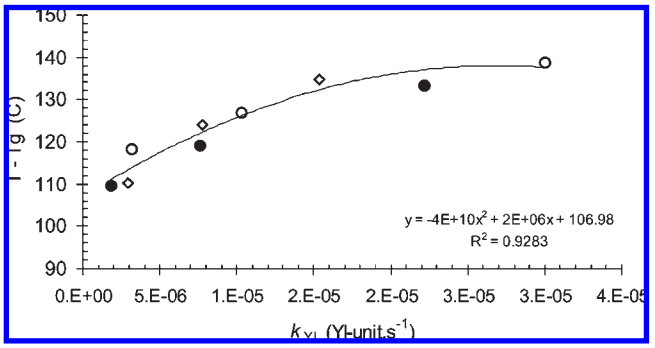

Figure 8. Plotting the difference between storage (T = 25 °C) and glass transition temperature (T_g) against rate constant of NEB development (k_{YI}) in HMP films (●) stored at 33.3, 57.7, or 75.2% RH (25 °C). The same is reported for gellan or deacylated (○) as well as for acylated−deacylated gellan (◇) mixed films (*11*).

and microstructural characteristics of the HMP network obtained (*55*).

Macromolecular Mobility. Relaxation of macromolecules assessed through thermal determination of T_g of HMP films showed a substantial decrease (≈23 °C) with the increment of the RH of storage or moisture content (**Table 2**). Pectin films stored at 25 °C were in an amorphous rubbery state, where macromolecular mobility increased dramatically with water content because of its plasticizing action, which is complemented with the effect of glycerol. There are not substantial differences between the T_g of pectin films and those of gellan (deacylated) or deacylated−acylated gellan mix films, as can be observed in **Figure 7B** (*11*). Moreover, the latter films showed the same T_g values when stored at 33.3 or 75.2% RH (**Figure 7B**), but the AA stability was different than the one of pectin (**Figure 5**). Hence, T_g (**Figure 7B**) could not completely justify the differences observed in AA stability (**Figure 5A**). A good correlation was observed (Pearson r = 0.911, $p < 0.001$; α: 0.05) when plotting the difference ($T - T_g$) as a function of browning rate constants (k_{YI}) in pectin films (**Figure 8**). A similar trend was observed for gellan-based films reported in a previous study (*11*). These relationships were not observed when plotting ($T - T_g$) against AA kinetic parameters. Because a better relationship of browning kinetics with the slowest water population was also found as indicated above, it is suggested that the browning development in solidlike systems like HMP films may be directly related to the hydroxyl groups of pectin macromolecules, that is, with the polymeric surfaces activated by water molecules closely adsorbed. Probably, the same occurs with all mentioned hydrophilic polymers when constituting films.

It was reported that homogenized and freeze-dried polymeric matrix model systems (gelatinized starch, maltodextrin, and polyvinylpyrrolidone with MW = 40000) containing a low concentration of added Maillard's reactants (D-glucose and L-lysine), which were further desiccated over P_2O_5 to "zero" % moisture and heated for 48 h at 90 °C, developed browning, although all of these model systems were well below their measured T_g (*56*). The authors suggested that the T_g should not be considered as an absolute threshold for stability with regard to NEB reactions. Leffler and Grunwald (*57*) indicated that some diffusion of reactants may even occur below T_g. In polymeric matrices, like in the above-mentioned polymeric systems, Maillard's reactants do not necessarily have to diffuse into them to accomplish browning, because chemicals were homogenized previously to freeze drying. Probably, all of these hydrophilic polymers may also be promoters of the browning reactions as active surfaces for water adsorption, and it is not possible to either completely "deactivate" them by the total elimination of the first monolayer of water adsorbed in the polymeric hydroxyl groups or by working below T_g.

Pure polymers show high T_g values (220−250 °C for dry cellulose, *58*) and some of them undergo thermal degradation without undergoing a glass transition. In our work, it was determined that a 25% glycerol aqueous solution showed a T_g value of −104.69 °C (onset). As a consequence, glycerol would be mainly responsible for the low magnitude of the T_g values showed by pectin-equilibrated films, as expected from a plasticizer (*59*). Probably, in our work, the measured T_g values corresponded to a glycerol-enriched phase in the pectin film (*60*, *61*). FTIR spectra herein determined may also support this statement. On the other hand, other small molecules present in the film formulation should be considered because they are also exerting additional plasticization (sorbate, AA), contributing to the low T_g temperatures in the systems (*62*, *63*). It has to be kept in mind that a polymer may show its backbone chain mobility increased because of plasticization, but this may not necessarily agree with the motions of water (or diluent) molecules, which become available to chemical reactions and microbial growth when these molecules are adequately mobile (*58*, *64*).

A higher increment of AA degradation and of the subsequent browning rate constant was observed in films stored at 75.2% RH with respect to 33.3 and 57.7%, a trend that correlates with an important increase in water mobility or T_2 (**Figure 6B**,**C**). The latter coincided with detection at −27.56 °C (peak) of some proportion of freezable bound water (*65*) by means of DSC studies only in pectin films equilibrated at 75.2% RH, a fact that might indicate that there was some proportion of less closely associated water with the polymer matrix or of water with special higher mobility at this RH condition, responsible for a faster AA destruction. The same was observed in previous works (*10*, *11*) with gellan-based films stored at the highest RH (75.2%).

Mechanical Performance of Films. It was determined in the large deformation scale and uniaxial condition at a constant cross-head speed of 5 mm/min. Tensile strength at rupture was calculated as the adequate parameter for comparison as recommended earlier by Ferry (*66*) for the tensile test. It can be seen in **Figure 9A** that deformation at rupture decreased with the increment of T_{2a}, the slowest water population of the total moisture contents of pectin films. Deformation of samples stored at 75.2% RH, that is, with the highest T_{2a} value, was significantly lower than at the other conditions. The increase in the moisture content with the RH of film storage, which led to higher T_{2a}, may allow the association of polymer units, which is facilitated by enhanced macromolecular mobility in the rubbery state (*67*), leading to lower deformation. It can also be suggested that penetration of water molecules into the pectin polymeric network may produce their constraint, evidenced by the inverse relationship between deformation-at-break and moisture content (**Figure 9A**).

Tensile strength at film failure decreased significantly as T_{2a} or water mobility increased in the film network (**Figure 9A**), as a consequence of water plasticization. The tensile strength parameter changed in a significant power relationship with the solid content of the pectin network (**Figure 9B**). It is known in the literature that the elastic modulus is a function of the polymer concentration and changes in a power ratio (*68*−*70*). As a consequence, it has been indicated that the elastic modulus is proportional to the cross-linking degree or polymer−polymer interactions, herein of physical origin (hydrogen bonds, hydrophobic interactions, electrostatic forces) at the junction zones. Therefore, plasticization produced a decrease in the tensile

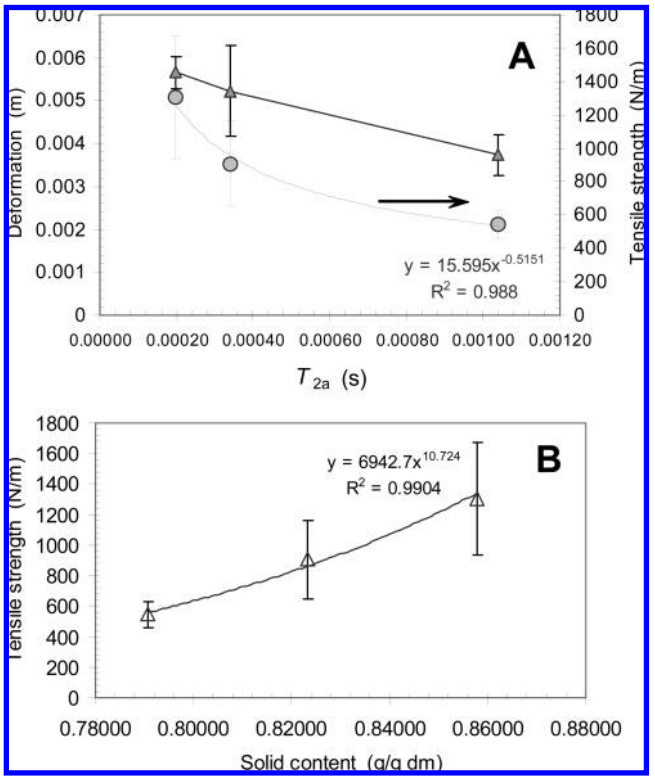

Figure 9. Deformation at rupture and tensile strength [calculated as the ratio between force (N) and deformation (m) at failure] against the spin−spin time constant T_{2a} of film samples (**A**). Tensile strength as a function of the solid content of pectin films equilibrated at each condition of storage RH (**B**). Error bars indicate SDs (n = 9).

strength of films from 1306 to 550 N/m as RH increased from 33.3 to 75.2% (**Figure 9B**).

A fractal dimension $D_f^{3d} = 2.90$ was derived from the exponent of the fitted power equation of tensile strength vs solid content (**Figure 9B**), which is in relation to the microstructural order of the network developed during film constitution (**Figure 10**). Atomic force microscopy images of the HMP films in the 1.0 μm × 1.0 μm scale (**Figure 10**) showed a homogeneous network, which seems constituted by aggregate "flocs" of a regular diameter, mainly 50−65 nm and other of 30 nm. The fractal dimension determined by the erosion dilatation method (EDM) on the atomic force microscopy images, like that observed in **Figure 10**, was D_{EDM} = 2.90. It is shown that the fractal dimension is sensitive to the spatial distribution of the particles in the network. The latter value was in agreement with the fractal dimension found from the tensile test of pectin films. Higher fractal dimensions occur in networks that are more ordered or, as in the present case, where larger flocs characterized the microstructure. The weak-link regime was herein considered to calculate the rheological fractal dimension. These results suggest that it is the links between the polymer flocs that yield under tension. Because each junction zone is a pillar of gel strength (*12*), the flocs observed in **Figure 10** would be related to each other through some short lateral aggregation of two or three alternating hydrophilic−hydrophobic channel junction zones, which are responsible for the ordered regions observed through X-ray diffraction: the trigonal unit cell with z = 13.0 Å as well as the hydrogen bonds (2.8 Å) that relate antiparallel helices through the remaining free carboxylic groups (27%). Consequently, disordered (hairy) regions may be those that look like elliptical spheroid flocs (**Figure 10**).

Gellan-based films reported in a previous study, formulated with either higher or similar ratios of glycerol to polymer than

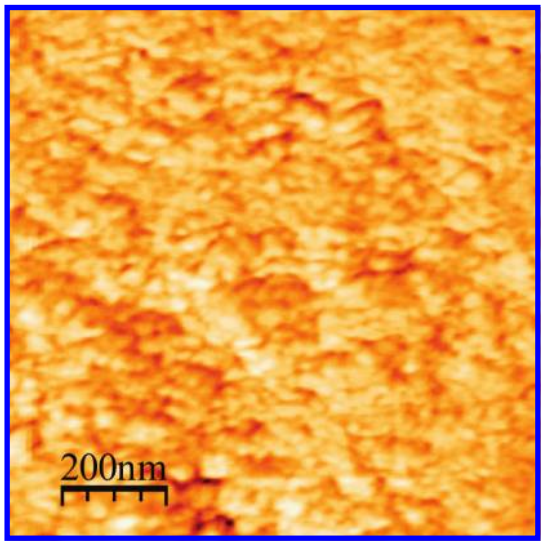

Figure 10. Atomic force microscopy image obtained from HMP films with a scan size of 1.0 μm × 1.0 μm.

pectin films, showed tensile strength values of 1400−1700 and 1700−2400 N/m, respectively (*11*). It can be concluded that the presence of a high frequency of methoxyl groups that leads to more transient junction zones in the pectin film network, in conjunction with a 14% (molar bases) of disordered regions that can dissipate the tensile stress, may lead to a less rigid macromolecular network than in the case of gellan networks (*13*). These events allowed lowering of the glycerol content even though a higher proportion of pectin polymer was used with respect to all gellan-based systems. Its microstructural organization in larger flocs where the links between them are weaker and yield under tension promoted less resistant networks in comparison to those developed through lateral or side-by-side aggregation of polymeric helices as occurred in the case of gellan-based films (*14*). At the same time, the less mobile population (T_{2a}) of water molecules seemed to be related with polymer plasticization in the pectin films.

In the present study, the AA stability and subsequent browning development depended on the water availability in the HMP film networks. This microstructure produced a better immobilization of water molecules in comparison with gellan-based films previously studied, leading to a higher AA retention and lower browning rate as well, at the two lowest RHs of storage. Mechanical testing of films in the large deformation scale developed the major compromise of water contents with the plasticization of the polymeric networks when stored at 33.3 or 57.7% RH, whereas film equilibration at 75.2% RH allowed detection of freezable bound water through DSC studies, which might not be compromised in plasticization but contributed to an important increment in water mobility (T_2) in the film microstructure and, hence, to the exponential increase in AA loss and subsequent browning development. This result, which was only observed when water was more available for reactions, might be attributed to the lower retention of water molecules in the HMP network at 75.2% RH of film equilibration. At this condition, disorder regions of this pectin network may not be adequately counterbalanced by junction zones constituted by alternating hydrophilic (water) and hydrophobic interactions, which are in addition disturbed by glycerol molecules. Therefore, water was less immobilized than in the acylated−deacylated gellan mix films, where lateral aggregation occurred, constituting a continuous branched fibrous network, although with some important degree of spatial hindering (*14*). Hence, it is suggested that disorder

regions (14% of the pectin used) should have to be distributed in a network developed from less transient junction zones like those electrostatically (calcium) mediated in the case of low methoxyl pectins, in order to accomplish sufficiently higher water immobilization in the whole network. Hence, AA loss and subsequent NEB development could be better controlled through the adequate selection of a polymer, in view of higher immobilization of water in the film network.

ABBREVIATIONS USED

HMP, high methoxyl pectin; AA, L-(+)-ascorbic acid; NEB, nonenzymatic browning; RH, relative humidity; $a_W°$, true water activity; YI, yellow index; SD, standard deviation; WVP, water vapor permeability; FTIR, Fourier transform infrared spectroscopy; NMR, nuclear magnetic resonance; T_{2a}, T_{2b}, spin−spin relaxation times with a and b subscripts indicating the two components of the relaxation process; $M(t)$, peak height of the spin−spin relaxation; M_1 and M_2, equilibrium magnetization in the spin−spin relaxation; λ, wavelength of the X-ray beam (Bragg's law); n, order of reflection, which was considered as 1 (Bragg's law); d (Å), distances between the planes of the crystals; A, system-dependent proportionality constant; $t_{1/2}$, half-life time of AA; t_2, the time for YI duplication; T_g, glass transition temperature; ν_{AA}, stechiometric coefficient for AA hydrolytic degradation reaction (here $\nu_{AA} = 1$); r_{AA}, AA reaction rate/unit volume at constant temperature; [AA], molar concentration of AA; [H_2O], molar concentration of water; k, rate constant of the second-order kinetics for AA hydrolytic degradation reaction; k_{AA}', rate constant of the pseudo first-order kinetics for AA hydrolytic degradation reaction; S_N2, bimolecular nucleophilic substitution mechanism; KGA, 2-keto-L-gulonic acid; GalA, D-galacturonic acid; Rha, rhamnose; Fuc, fucose; Ara, arabinose; Xyl, xylose; Man, manose; Gal, galactose; Glc, glucose.

ACKNOWLEDGMENT

We are grateful to Graciela Guananja (CP Kelco) for her attention with respect to our needs for CP Kelco pectins that were provided without cost by the company, Dr. Gustavo A. Monti and Belén Franzoni of the LANAIS (Laboratorio Nacional de Investigación y Servicios) for NMR of solid materials, and the Facultad de Matemática, Astronomía y Física (FaMAF), Universidad Nacional de Córdoba, Argentina, for their help with the NMR analysis.

LITERATURE CITED

(1) Rhim, J. W.; Hong, S. I.; Park, H. M.; Ng, P. K. W. Preparation and characterization of chitosan-based nanocomposite films with antimicrobial activity. *J. Agric. Food Chem.* **2006**, *54*, 5814–5822.

(2) Butler, B. L.; Vergano, P. J.; Testin, R. F.; Bunn, J. M.; Wiles, J. L. Mechanical and barrier properties of edible chitosan films as affected by composition and storage. *J. Food Sci.* **1996**, *61* (5), 953 –956.

(3) Onyechi, U. A.; Judd, P. A.; Ellis, P. R. African plant foods rich in non-starch polysaccharides reduce postprandial blood glucose and insulin concentrations in healthy human subjects. *Br. J. Nutr.* **1998**, *80*, 419–428.

(4) Funami, T.; Kataoka, Y.; Omoto, T.; Goto, Y.; Asai, I.; Nishinari, K. Effects of non-ionic polysaccharides on the gelatinization and retrogradation behavior of wheat starch. *Food Hydrocolloids* **2005**, *19* (1), 1–13.

(5) Fennema, O. R.; Kamper, S. L.; Kester, J. J. Method for making an edible film and for retarding water transfer among multi-component food products. U.S. Patent 4915971, publication date 4/10/**1990**.

(6) Sanjurjo, K.; Flores, S.; Gerschenson, L. N.; Jagus, R. Study of the performance of nisin supported in edible films. *Food Res. Int.* **2006**, *39* (6), 749–754.

(7) Chen, L.; Remondetto, G. E.; Subirade, M. Food protein-based materials as nutraceutical delivery systems. *Trends Food Sci. Technol* **2006**, *17*, 272–283.

(8) Durschlag, M. E.; Kehoe, G. S. Edible film for transmucosal delivery of nutritional supplements. U.S. Patent Application 20070087036 (Kind Code: A1), publication date 4/19/**2007**.

(9) Liu, Y.; Chakrabartty, S.; Alocilja, E. Fundamental building blocks for molecular biowire based forward error-correcting biosensors. *Nanotechnology* **2007**, *18*, 1–6.

(10) León, P. G.; Rojas, A. M. Gellan gum films as carriers of L-(+)-ascorbic acid. *Food Res. Int.* **2007**, *40*, 565–575.

(11) León, P. G.; Lamanna, M. E.; Gerschenson, L. N.; Rojas, A. M. Influence of composition of edible films based on gellan polymers on L-(+)-ascorbic acid stability. *Food Res. Int.* **2008**, *41* (6), 667–675.

(12) Chandrasekaran, R. X-ray diffraction of food polysaccharides. *Adv. Food Nutr. Res.* **1998**, *42*, 131−210 (131−137, 167−172, 185−191).

(13) Morris, V. J.; Mackie, A. R.; Wilde, P. J.; Kirby, A. R.; Mills, E. C. N.; Gunning, A. P. Atomic force microscopy as a tool for interpreting the rheology of food biopolymers at the molecular level. *Lebensm.-Wiss. Technol.* (*LWT*) **2001**, *34* (1), 3–10.

(14) León, P. G.; Chillo, S.; Conte, A.; Gerschenson, L. N.; Del Nobile, M. A.; Rojas, A. M. Rheological characterization of deacylated/acylated gellan films carrying L-(+)-ascorbic acid. *Food Hydrocolloids* **2009**, *23*, 1660–1669.

(15) Lapasin, R.; Pricl, S. *Rheology of Industrial Polysaccharides. Theory and Applications*; Blackie Academic and Professional, Chapman & Hall: Glasgow, United Kingdom, 1995; pp 85−103.

(16) Pérez, S.; Rodríguez-Carvajal, M. A.; Doco, T. A complex plant cell wall polysaccharide: Rhamnogalacturonan II. A structure in quest of a function. *Biochimie* **2003**, *85*, 109–121.

(17) Fissore, E. N.; Ponce, N. M. A.; Wider, E. A.; Stortz, C. A.; Gerschenson, L. N.; Rojas, A. M. Commercial cell wall hydrolytic enzymes for producing pectin-enriched products from butternut (*Cucurbita moschata*, Duchesne ex Poiret). *J. Food Eng.* **2009**, *93* (3), 293–301.

(18) ASTM D 1925. *Standard Test Method for Yellowness Index of Plastics*; American Society for Testing and Materials: Philadelphia, 1988.

(19) *Mettler DSC User's Manual*; Mettler-Toledo GmbH: Schwerzenbach, Switzerland, **1997**; pp 42−45.

(20) Gennadios, A.; Weller, C. L.; Gooding, C. H. Measurement errors in water vapor permeability of highly permeable, hydrophylic edible films. *J. Food Eng.* **1994**, *21*, 395–409.

(21) Horcas, I.; Fernandez, R.; Gomez-Rodriguez, J. M.; Colchero, J. WSXM: A software for scanning probe microscopy and a tool for nanotechnology. *Rev. Sci. Instrum.* **2007**, *78*, 013705.

(22) Shih, W.; Shih, W. Y.; Kim, S.; Liu, J.; Aksay, I. A. Scaling behavior of the elastic properties of colloidal gels. *Phys. Rev. A* **1990**, *42*, 4772 –4779.

(23) Russ, J. C. *The Image Processing Handbook*, 4th ed.; CRC Press: Boca Raton, FL, 2002.

(24) Sokal, R. R.; Rohlf, J. B. Biometry. *The Principles and Practice of Statistics in Biological Research*; WH Freeman and Company: San Francisco, 2000; pp 253−380.

(25) Bancroft, H. *Introducción a la Bioestadística*; EUDEBA: Editorial Universitaria de Buenos Aires: Ciudad de Buenos Aires, Argentina, 1986; pp 180−188.

(26) Braccini, I.; Pérez, S. Molecular basis of Ca^{2+}-induced gelation in alginates and pectins: the egg box model revisited. *Biomacromolecules* **2001**, *2*, 1089–1096.

(27) Oakenfull, D.; Scott, A. Hydrofobic interaction in the gelation of high methoxyl pectins. *J. Food Sci.* **1984**, *49*, 1093–1098.

(28) Fang, Y.; Al-Assaf, S.; Phillips, G. O.; Nishinari, K.; Funami, T.; Williams, P. A. Binding behavior of calcium to polyuronates: Comparison of pectin with alginate. *Carbohydr. Polym.* **2008**, *72*, 334–341.

(29) Chandrasekaran, R.; Puigjaner, L. C.; Joyce, K. L.; Arnott, S. Cation interactions in gellan: an X-ray study of the potassium salt. *Carbohydr. Res.* **1988**, *181*, 23–40.

(30) Gnanasambandam, R.; Proctor, A. Determination of pectin degree of esterification by diffuse reflectance Fourier transform infrared spectroscopy. *Food Chem.* **2000**, *68* (3), 327–332.

(31) Wilson, R. H.; Smith, A. C.; Kačuráková, M.; Saunders, P. K.; Wellner, N.; Waldron, K. W. The mechanical properties and molecular dynamics of plant cell wall polysaccharides studied by Fourier-transform infrared spectroscopy. *Plant Physiol*. **2000**, *124*, 397–405.
(32) McCann, M. C.; Hammouri, M.; Wilson, R.; Belton, P.; Roberts, K. Fourier transform infrared microspectroscopy is a new way to look at plant cell walls. *Plant Physiol*. **1992**, *100*, 1940–1947.
(33) Coimbra, M. A.; Barros, A.; Barros, M.; Rutledge, D. N.; Delgadillo, I. FTIR spectroscopy as a tool for the analysis of olive pulp cell-wall polysaccharide extracts. *Carbohydr. Res*. **1999**, *317*, 145–154.
(34) Alonso-Simón, A.; Encina, A. E.; García-Angulo, P.; Álvarez, J. M.; Acebes, J. L. FTIR spectroscopy monitoring of cell wall modifications during the habituation of bean (*Phaseolus vulgaris* L.) callus cultures to dichlobenil. *Plant Sci*. **2004**, *167* (6), 1273–1281.
(35) Thygesen, L. G.; Løkke, M. M.; Micklander, E.; Engelsen, S. B. Vibrational microspectroscopy of food. Raman vs. FT-IR. *Trends Food Sci. Technol*. **2003**, *14* (1−2), 50–57.
(36) Yang, J.; Yu, J.; Ma, X. Study on the properties of ethylenebisformamide and sorbitol plasticized corn starch (ESPTPS). *Carbohydr. Polym*. **2006**, *66*, 110–116.
(37) Dashnau, J. L.; Nucci, N. V.; Sharp, K. A.; Vanderkooi, J. M. Hydrogen bonding and the cryoprotective properties of glycerol/water mixtures. *J. Phys. Chem. B* **2006**, *110*, 13670–13677.
(38) Mathlouthi, M. Water content, water activity, water structure and the stability of foodstuffs. *Food Control* **2001**, *12* (7), 409–417.
(39) Shellhammer, T. H.; Krochta, J. M. Whey protein emulsion film performance as affected by lipid type and amount. *J. Food Sci*. **1997**, *62* (2), 390–394.
(40) Yang, L.; Paulson, A. T. Mechanical and water vapour barrier properties of edible gellan films. *Food Res. Int*. **2000**, *33* (7), 563–570.
(41) Kasapis, S. Recent advances and future challenges in the explanation and exploitation of the network glass transition of high sugar/biopolymer mixtures. *Crit. Rev. Food Sci. Nutr*. **2008**, *48* (2), 185–203.
(42) Saguy, I.; Mizrahi, S.; Villota, R.; Karel, M. Accelerated method for determining the kinetic model of ascorbic acid loss during dehydration. *J. Food Sci*. **1978**, *43*, 1861–1864.
(43) Rojas, A. M.; Gerschenson, L. N. Ascorbic acid destruction in aqueous model systems: An additional discussion. *J. Sci. Food Agric*. **2001**, *81* (15), 1433–1439.
(44) Torregrosa, F.; Esteve, M. J.; Frígola, A.; Cortés, C. Ascorbic acid stability during refrigerated storage of orange−carrot juice treated by high pulsed electric field and comparison with pasteurized juice. *J. Food Eng*. **2006**, *73* (4), 339–345.
(45) Labuza, T.; Baisier, W. M. The kinetics of nonenzymatic browning. In *Physical Chemistry of Foods*; Schwartzberg, H., Hartel, R., Eds.; Marcel Dekker: New York, 1992; pp 595−649.
(46) Kurata, T.; Sakurai, Y. Degradation of L-ascorbic acid and mechanism of non-enzymic browning reaction. Part II. *Agric. Biol. Chem*. **1967**, *31*, 170–176.
(47) Morrison, R. T.; Boyd, R. N. *Química Orgánica*; Addison-Wesley Iberoamericana, S. A.: Wilmington, DE, 1990; pp 190, 211, 233.
(48) Kou, Y.; Dickinson, L. C.; Chinachoti, P. Mobility characterization of waxy corn starch using wide-line ^{1}H nuclear magnetic resonance. *J. Agric. Food Chem*. **2000**, *48* (11), 5489–5495.
(49) Vittadini, E.; Chinachoti, P. Effect of physico-chemical and molecular mobility parameters on *Staphylococcus aureus* growth. *Int. J. Food Sci. Technol*. **2003**, *38* (8), 841–847.
(50) Chen, P. L.; Long, Z.; Ruan, R.; Labuza, T. P. Nuclear resonance studies of water mobility in bread during storage. *Lebensm.-Wiss. Technol*. (*LWT*) **1997**, *30*, 178–183.
(51) Kerr, W. L.; Wicker, L. NMR proton relaxation measurements of water associated with high methoxy and low methoxy pectins. *Carbohydr. Polym*. **2000**, *42* (2), 133–141.
(52) Corain, B.; Zecca, M.; Jeřábek, K. Catalysis and polymer networks-the role of morphology and molecular accessibility. *J. Mol. Catal. A: Chem*. **2001**, *177*, 3–20.
(53) Flores, S.; Famá, L.; Rojas, A. M.; Goyanes, S.; Gerschenson, L. N. Physical properties of tapioca-starch edible films: Influence of filmmaking and potassium sorbate. *Food Res*. **2007**, *40* (2), 257–265.
(54) Oosterveld, A.; Beldman, G.; Schols, H. A.; Voragen, A. G. J. Characterization of arabinose and ferulic acid rich pectic polysaccharides and hemicelluloses from sugar beet pulp. *Carbohydr. Res*. **2000**, *328*, 185–197.
(55) Willats, W. G. T.; Knox, J. P.; Mikkelsen, D. Pectin: New insights into an old 623 polymer are starting to gel. *Trends Food Sci. Technol*. **2006**, *17*, 97–104.
(56) Schebor, C.; Buera, M. P.; Karel, M.; Chirife, J. Color formation due to non-enzymatic browning in amorphous, glassy, anhydrous, model systems. *Food Chem*. **1999**, *65* (4), 427–432.
(57) Leffler, J.; Grunwald, E. Extrathermodynamic analysis of enthalpy and entropy changes. In *Rates and Equilibria of Organic Reactions*; John Wiley and Sons: New York, 1963; pp 315−402.
(58) Vittadini, E.; Dickinson, L. C.; Chinachoti, P. ^{1}H and ^{2}H NMR mobility in cellulose. *Carbohydr. Polym*. **2001**, *46* (1), 49–57.
(59) Sothornvit, R.; Krochta, J. M. Plasticizers in edible films and coatings. In *Innovations in Food Packaging*; Jung, H. H., Ed.; Elsevier: Oxford, 2005; Chapter 23, pp 404−410.
(60) Forsell, P. M.; Mikkila, J. M.; Moates, G. K.; Parker, R. Phase and glass transition behaviour of concentrated barley starch−glycerol mixtures, a model for thermoplastic starch. *Carbohydr. Polym*. **1997**, *34*, 275–282.
(61) Wilhelm, H. M.; Sierakowski, M. R.; Souza, G. P.; Wypych, F. Starch films reinforced with mineral clay. *Carbohydr. Polym*. **2003**, *52*, 101–110.
(62) Chartoff, R. P. *Thermal Characterization of Polymeric Materials*; Turi, E. A., Ed.; Academic Press: United States, 1981; Vol. *1*, pp 531−543.
(63) Famá, L.; Rojas, A. M.; Goyanes, S.; Gerschenson, L. N. Mechanical properties of tapioca-starch edible films containing sorbates. *Lebensm.-Wiss. Technol*. (*LWT*) **2005**, *38*, 631–639.
(64) Li, S.; Dickinson, L. C.; Chinachoti, P. Mobility of unfreezable and freezable water in waxy corn starch by ^{2}H and ^{1}H NMR. *J. Agric. Food Chem*. **1998**, *46*, 62–71.
(65) Hatakeyama, H.; Hatakeyama, T. Interaction between water and hydrophilic polymers. *Thermochim. Acta* **1998**, *308*, 3–22.
(66) Ferry, J. D. *Viscoelastic Properties of Polymers*; John Wiley and Sons, Inc.: United States, 1980; Vol. *1*.
(67) Pittia, P.; Sacchetti, G. Antiplasticization effect of water in amorphous foods. A review. *Food Chem*. **2008**, *106*, 1417–1427.
(68) Mc Evoy, H.; Ross-Murphy, S. B.; Clark, A. H. Large deformation and ultimate properties of biopolymer gels: 1. Single biopolymer component systems. *Polymer* **1985**, *26*, 1483–1492.
(69) Grassi, M.; Lapasin, R.; Pricl, S. A study of the rheological behavior of scleroglucan weak gel systems. *Carbohydr. Polym*. **1996**, *29*, 169–181.
(70) Narine, S. S.; Marangoni, A. G. Fractal nature of fat crystal networks. *Phys. Rev. E* **1999**, *59*, 1908–1920.

Received December 26, 2008. Revised manuscript received June 12, 2009. Accepted July 2, 2009. This research work received financial support from the Universidad de Buenos Aires (UBA), The National Agency for Promotion of Science and Technology (ANPCyT), and National Scientific and Technical Research Council (CONICET).